

Lattice location of implanted Ag in Si

U. Wahl ^(a), J.G. Correia ^{(b), (c)}, A. Vantomme ^(a) and the ISOLDE collaboration ^(c)

^(a) Instituut voor Kern- en Stralingsfysica, Katholieke Universiteit Leuven,
Celestijnenlaan 200 D, B-3001 Leuven, Belgium

^(b) Instituto Tecnológico e Nuclear, P-2685 Sacavém, Portugal

^(c) CERN-EP, CH-1211 Genève 23, Switzerland

Abstract

The lattice location of implanted silver in Si was studied by means of the emission channeling technique. Following 60 keV room temperature implantation of radioactive ^{111}Ag at a dose of $2\text{-}3\times 10^{12}\text{ cm}^{-2}$, we identify around 30% of Ag on near-substitutional sites ($\approx 0.45\text{ \AA}$ from ideal S-sites). Upon annealing at 200-300°C, the fraction on near-S sites reaches a maximum around 60-80%. For higher annealing temperatures it decreases again and at 600°C Ag starts to diffuse out of the Si samples. We estimate the activation energy for the dissociation of near-substitutional Ag to be 1.8-2.2 eV. The experimental results are compared to those of Cu in Si, and common features and characteristic differences in the behavior of the two group 1B metals are discussed.

PACS codes: 61.72.-y, 61.72.Tt, 61.72.Yx, 61.85.+p

Keywords: lattice location, ion implantation, emission channeling, silicon, transition metals

Introduction

Silver is well known to introduce various deep centers into silicon [1-3]. The two most prominent levels are an acceptor-type level, Ag(A), at an energy position $E_C-0.54\text{ eV}$ below the conduction band, and a donor-type level, Ag(D), at $E_V+0.34\text{ eV}$ above the valence band. The Ag(D) level could be assigned by means of photoluminescence (PL) [4,5] and infrared absorption spectroscopy [6] to a defect of C_{2v} or lower symmetry, and was suggested to be neutral substitutional Ag_S^0 . Electron paramagnetic resonance (EPR) measurements have identified at least 8 different Ag-related centers in Si, six of them are supposed to be due to pairs of Ag with other impurities or with itself [7-9]. Two centers, however, named NL56 and NL42 have been suggested to consist of substitutional Ag_S^0 and tetrahedral interstitial Ag_i^0 , respectively. While the NL56 center exhibited tetragonal (C_{2v}) or lower symmetry, indicating a displaced substitutional position of Ag, the NL42 center was the only one found to have tetrahedral (T_d) symmetry.

It is well known that Ag, like other transition metals, is gettered by highly damaged regions [10,11] or voids [12] in Si. Direct evidence on the exact lattice sites of Ag in Si is scarce, however. Rutherford Backscattering experiments [13] following 200-keV implantation of $1.5\times 10^{15}\text{ cm}^{-2}$ Ag and annealing at 550°C only showed that the silver atoms were incorporated in an amorphized region.

We have recently studied the lattice sites and stability of ion implanted Cu in Si by means of the emission channeling technique [14-16]. In this contribution we present lattice location experiments on ^{111}Ag , and compare the results for the two 1B transition metals.

Experimental

60 keV beams of radioactive ^{111}Ag ($t_{1/2}=7.45\text{ d}$) isotopes were produced at the ISOLDE facility at CERN by means of 1-GeV proton induced nuclear fission from UC_2 targets, chemically selective laser ionization and mass separation [17]. Three Si samples were implanted, all at room temperature, one *p*-type B-doped Czochralski (CZ) grown sample (resistivity 0.17-0.23 Ωcm , $\langle 100 \rangle$ surface, implanted dose $2.6\times 10^{12}\text{ cm}^{-2}$, sample A), one *p*-Si:B FZ (10-20 Ωcm , $\langle 100 \rangle$, $2.9\times 10^{12}\text{ cm}^{-2}$, sample B) and one *n*-Si:P FZ (700-1300 Ωcm , $\langle 111 \rangle$, $3.1\times 10^{12}\text{ cm}^{-2}$, sample C). Emission channeling [18] makes use of the fact that charged particles emitted from radioactive isotopes in single crystals experience channeling or blocking effects along low-index crystal directions. This leads to an anisotropic particle emission yield from the crystal surface which depends in a characteristic way on the lattice sites occupied by the emitter atoms and is recorded by means of a position sensitive detector. For the isotope ^{111}Ag , channeling patterns were extracted for the integral β^- spectrum above 50 keV up to the end point energy of 1041 keV.

In order to deduce the Ag lattice location from the β^- emission patterns we have carried out computer simulations of β^- emission yields for a variety of sites. The concept of electron emission channeling simulations

is based on the dynamical theory of electron diffraction and is described in detail in Ref. [18]. To approximate the continuous β^- energy spectrum, simulations were done for electron energies from 50 keV to 800 keV in steps of 25 keV, and from 850 keV to 1000 keV in steps of 50 keV. The results were averaged according to the spectral β^- distribution of ^{111}Ag [19]. We calculated characteristic two-dimensional patterns of electron emission probability within a range of $\pm 3^\circ$ around the $\langle 100 \rangle$, $\langle 111 \rangle$ and $\langle 110 \rangle$ directions in steps of $\Delta x = \Delta y = 0.05^\circ$ for S, T, hexagonal interstitial (H), bond center (BC), anti bonding (AB), split $\langle 100 \rangle$ (SP) and the so-called Y and C sites, as well as $\langle 111 \rangle$ and $\langle 100 \rangle$ displacements between these sites. The location of the sites is given in Refs. [14]. Quantitative information on the position of ^{111}Ag was then obtained by comparing the fit of simulated patterns to the observed yields. The fit procedures used for this purpose, as well as further experimental details, are described in Refs. [14-16,20].

Results and discussion

Figures 1(a), 1(b) and 1(c) show the $\langle 111 \rangle$, $\langle 100 \rangle$ and $\langle 110 \rangle$ β^- emission channeling patterns from sample C following room temperature implantation of ^{111}Ag and annealing at 200°C for 10 minutes. From the fact that channeling effects are observed along all major crystalline axes and planes it is obvious that the majority of Ag atoms must occupy substitutional (S) sites or sites which are close to the substitutional positions. The best fit results of simulated patterns to the experimental yields [Figs. 1(d), 1(e) and 1(f)] were obtained for lattice sites that are displaced by $0.45(5) \text{ \AA}$ along $\langle 111 \rangle$ directions from the substitutional towards the bond center (BC) position. The corresponding near- substitutional Ag fractions were 64% for the $\langle 111 \rangle$, 60% for the $\langle 100 \rangle$, and 65% for the $\langle 110 \rangle$ pattern, the remainder of Ag occupying random sites. Somewhat worse fits were obtained if the Ag was displaced along $\langle 111 \rangle$ from S to AB sites instead of to BC, or along $\langle 100 \rangle$ from S to SP sites. While the displacement of Ag from ideal substitutional sites is obvious from our results and the S \rightarrow BC sites resulted in the best fit, we cannot exclude the possibility that the displacement might occur along higher index directions than $\langle 111 \rangle$ or $\langle 100 \rangle$, or that we have a mixture of several sites with similar displacements. We also tested for additional fractions of Ag on other lattice sites, however, with the possible exception of tetrahedral interstitial T sites, which will be further discussed below, this resulted only in insignificant improvements in the quality of fit.

Figure 2 summarizes the lattice location results from all three investigated Si samples as a function of annealing temperature, and compares them to typical results for Cu in low-doped Si. In the as-implanted state, the near-substitutional fraction of Ag (30-35%) is lower than in the case of Cu (75-80%), but increases upon annealing to $200\text{-}300^\circ\text{C}$ to values around 60-80%. A possible reason for this is the higher damage density following implantation of the heavier isotope ^{111}Ag in comparison to ^{67}Cu (note that the implanted doses were similar). Most of the damage anneals around $200\text{-}300^\circ\text{C}$, resulting in the majority of Ag occupying, within measurement precision, the same displaced substitutional lattice sites as Cu. Upon annealing at higher temperatures, the near-substitutional fraction of Ag decreases continuously in a similar way as was seen for Cu. However, in contrast to ^{67}Cu , the $\langle 110 \rangle$ patterns from ^{111}Ag measured following annealing at 400°C and 500°C could be fitted significantly better if an additional fraction on tetrahedral interstitial T sites was allowed (note that T sites can not be distinguished from S sites by means of the $\langle 100 \rangle$ or $\langle 111 \rangle$ patterns). Consequently we have allowed for a fraction on T sites in all other fits, however, as can be seen from Fig. 2, except following annealing at 400°C and 500°C , the T fractions are small and close to the measurement error. In sample B the near-S fraction of Ag decreased faster than in sample A, but more measurements will be needed in order to assess whether this trend is due to the *n*- or *p*-type doping or the fact that sample B was FZ and sample A CZ material. Following annealing at 600°C , 30-50% of ^{111}Ag diffused out of the Si samples, as was obvious from the fact that significant radioactivity could be detected on the sample holder. This is also in contrast to Cu, which did not show any out-diffusion but was found to diffuse mainly to the bulk of the Si samples at 600°C .

We have estimated the activation energy E_A for the dissociation of near substitutional Ag using two simple models that have been outlined in detail in Ref. [15]. The first estimate is based on a one-step model which assumes that one successful jump of Ag is sufficient to completely dissociate the defect and which neglects re-trapping. In this case we deduce $E_A = 2.2 \text{ eV}$. The second model considers the possibility that all vacancies created during implantation act as traps for Ag, and yields the lower value of $E_A = 1.8 \text{ eV}$. These values may be compared with the activation energies for Ag diffusion in crystalline and amorphous Si that are given in the literature. As was to be expected, the dissociation energy for near-substitutional Ag is significantly higher than the interstitial migration energy of Ag in crystalline Si, which was estimated to be around 1.15 eV [21], but similar to the activation energy for Ag diffusion in amorphous Si, which is 1.6 eV [11].

It is interesting to compare the stability of near-substitutional Ag with the annealing behavior of the Ag DLTS levels described in the literature [2,3]. For Ag-diffused and quenched Si, the concentration of the Ag(A) level did not change at all after annealing up to 386°C . Since our experiments show directly that near-S Ag is increasingly unstable above 300°C , the proposed assessment of Ag(A) with substitutional Ag in Ref. [3]

seems questionable. The Ag(D) level, on the other hand, was only stable up to 300°C and decreased in intensity by a factor of two following annealing at 386°C. The similarity of the annealing behavior of the Ag(D) level with the near-substitutional Ag in our experiments, together with the fact that the concentration of Ag(D) increased upon irradiation with α particles [3], rather points towards the explanation that Ag(D) involves substitutional Ag, resulting from a reaction of Ag with vacancy-like defects. This would also be in accordance with the identification suggested for Ag(D) by the EPR and optical measurements mentioned above.

Conclusions

We have shown directly that Ag occupies near-substitutional lattice sites following implantation into Si. Upon annealing to 200-300°C the preferred lattice site of implanted Ag was found to be identical to the one of Cu, showing that incorporation on displaced substitutional sites is a common phenomenon for both 1B metals. The dissociation energies of near-substitutional Ag and Cu in low-doped Si were also found to be similar. Our experiments further indicate that the formation of near-substitutional Ag is, at least partly, responsible for the radiation damage gettering effect of Ag in Si.

Acknowledgments

This work was partially funded by the TMR-LSF program of the European Union, and by the FCT, Portugal (project CERN/c/FIS/15180/99).

References

- [1] N. Baber, H.G. Grimmeis, M. Klevermann, P. Omling, and M. Zafar Iqbal, *J. Appl. Phys.* 62 (1987) 2853.
- [2] A. Ali, M. Zafar Iqbal, and N. Baber, *J. Appl. Phys.* 77 (1995) 3315.
- [3] A. Ali, N. Baber, and M. Zafar Iqbal, *J. Appl. Phys.* 77 (1995) 5050.
- [4] N.T. Son, M. Singh, J. Dalfors, B. Monemar, and E. Janzén, *Phys. Rev. B* 49 (1994) 17428.
- [5] M. Zafar Iqbal, G. Davies, and E.C. Lightowlers, *Mater. Sci. Forum.* 143-147 (1994) 773.
- [6] J. Olajos, M. Klevermann, and H.G. Grimmeis, *Phys. Rev. B* 38 (1988) 10633.
- [7] N.T. Son, V.E. Kustov, T. Gregorkiewicz, and C.A.J. Ammerlaan, *Phys. Rev. B* 46 (1992) 4544.
- [8] N.T. Son, T. Gregorkiewicz, and C.A.J. Ammerlaan, *J. Appl. Phys.* 73 (1993) 1797.
- [9] P.N. Hai, T. Gregorkiewicz, C.A.J. Ammerlaan, and D.T. Don, *Phys. Rev. B* 56 (1997) 4614.
- [10] R.G. Wilson, *J. Appl. Phys.* 60 (1986) 2810.
- [11] S. Coffa, J.M. Poate, D.C. Jacobson, W. Frank, and W. Gustin, *Phys. Rev. B* 45 (1992) 8355.
- [12] A. Kinomura, J.S. Williams, J. Wong-Leung, and M. Petravic, *Appl. Phys. Lett.* 72 (1998) 2713.
- [13] S.U. Campisano, G. Foti, P. Baeri, M.G. Grimaldi, and E. Rimini, *Appl. Phys. Lett.* 37 (1980) 719.
- [14] U. Wahl, J.G. Correia, A. Vantomme, G. Langouche, and the ISOLDE collaboration, *Physica B* 273-274 (1999) 367.
- [15] U. Wahl, J.G. Correia, A. Vantomme, G. Langouche, and the ISOLDE collaboration, *Phys. Rev. Lett.* 84 (2000) 1495.
- [16] U. Wahl, A. Vantomme, G. Langouche, J.P. Araújo, L. Peralta, J.G. Correia, and the ISOLDE collaboration, *Appl. Phys. Lett.* 77 (2000) 2142.
- [17] Y. Jading, R. Catherall, V.N. Fedoseyev, A. Jokinen, O.C. Jonson, T. Kautzsch, I. Klöckl, K.L. Kratz, E. Kugler, J. Lettry, V.I. Mishin, H.L. Ravn, F. Scheerer, O. Tengblad, P. Van Duppen, W.B. Walters, A. Wöhr, and the ISOLDE collaboration, *Nucl. Instr. Meth. Phys. Res. B* 126 (1997) 76.
- [18] H. Hofsäss and G. Lindner, *Phys. Rep.* 210 (1991) 121.
- [19] S.Y.F. Chu, L.P. Ekström and R.B. Firestone, WWW Table of Radioactive Isotopes, database version of 28.2.1999, <http://nucleardata.nuclear.lu.se/toi/>.
- [20] U. Wahl, *Hyperfine Interactions* 129 (2000) 349.
- [21] F. Rollert, N.A. Stolwijk, and H. Mehrer, *J. Phys. D: Appl. Phys.* 20 (1987) 1148.

Fig. 1, U. Wahl et al

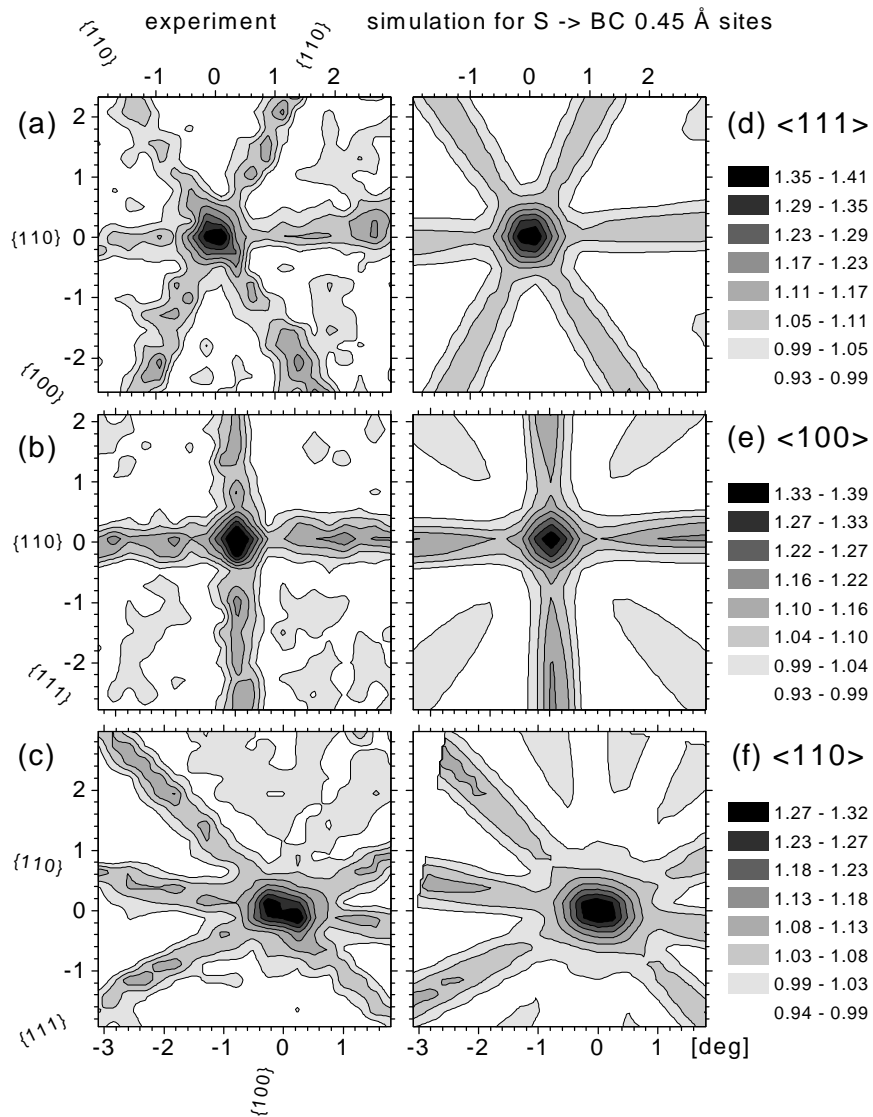


Fig. 1. (a)-(c): $\langle 111 \rangle$, $\langle 100 \rangle$ and $\langle 110 \rangle$ channeling patterns from ^{111}Ag following room temperature implantation into $n\text{-Si:P}$ FZ (sample C) and annealing at 200°C . (d)-(f): Best fits of simulated patterns to the experimental yields, corresponding to 64%, 60, and 65% on sites which are displaced by $0.45(5)$ Å from S to BC.

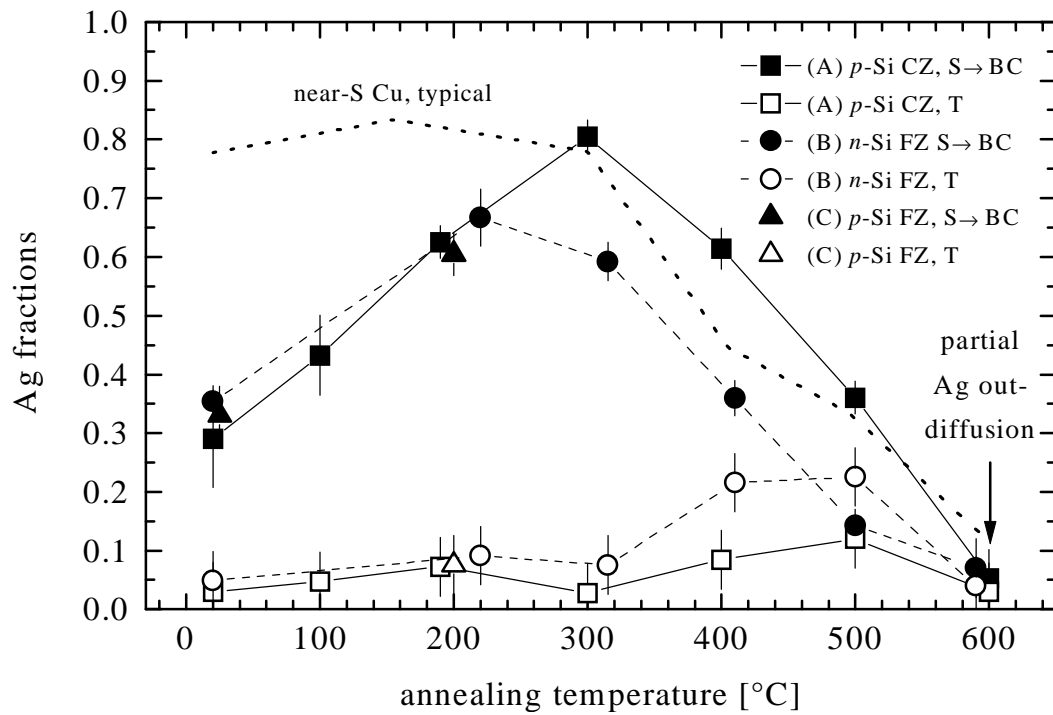


Fig. 2, U. Wahl et al

Fig. 2. Fractions of implanted ^{111}Ag on near-substitutional (S \rightarrow BC) and tetrahedral interstitial (T) sites as function of isochronal (10 min) annealing temperature. In comparison, the dotted line shows a typical result for implanted ^{67}Cu in low-doped Si [Wahl 00].